



# Capillary Microreactor for Initial Screening of Three Amine-Based Solvents for CO<sub>2</sub> Absorption, Desorption, and Foaming

Anchu Ashok<sup>1</sup>, Jaafar Ballout<sup>2</sup>, Abdelbaki Benamor<sup>3,4</sup> and Ma'moun Al-Rawashdeh<sup>1\*</sup>

<sup>1</sup>Department of Chemical Engineering, Texas A&M University at Qatar, Doha, Qatar, <sup>2</sup>Baha and Walid Bassatne Department of Chemical Engineering and Advanced Energy, American University of Beirut, Beirut, Lebanon, <sup>3</sup>Gas Processing Center, College of Engineering, Qatar University, Doha, Qatar, <sup>4</sup>Department of Chemical Engineering, College of Engineering, Qatar University, Doha, Qatar

## OPEN ACCESS

### Edited by:

Jun Yue,  
University of Groningen, Netherlands

### Reviewed by:

Jean-Marc Commenge,  
Université de Lorraine, France  
Rufat Abiev,  
Saint Petersburg State Institute of  
Technology, Russia

### \*Correspondence:

Ma'moun Al-Rawashdeh  
mamoun.al-rawashdeh@  
qatar.tamu.edu

### Specialty section:

This article was submitted to  
Microfluidic Engineering and Process  
Intensification,  
a section of the journal  
Frontiers in Chemical Engineering

**Received:** 19 September 2021

**Accepted:** 17 May 2022

**Published:** 01 June 2022

### Citation:

Ashok A, Ballout J, Benamor A and  
Al-Rawashdeh M (2022) Capillary  
Microreactor for Initial Screening of  
Three Amine-Based Solvents for CO<sub>2</sub>  
Absorption, Desorption, and Foaming.  
Front. Chem. Eng. 4:779611.  
doi: 10.3389/fceng.2022.779611

Microreactor is a very attractive laboratory device for screening conditions and solvents in an efficient, safe and fast manner. Most reported work on microreactors for CO<sub>2</sub> capturing deals with absorption and mass transfer performance with a limited number of studies on solvent regeneration. For the first time, foaming, which is a major operational challenge of CO<sub>2</sub> capturing is being studied in combination with absorption and desorption in a capillary microreactor setup. To demonstrate the setup capabilities, three known amine-based solvents (MEA, MDEA, and AMP) were selected for the screening and evaluation studies. MEA had the highest CO<sub>2</sub> absorption efficiency while MDEA had the lowest one. CO<sub>2</sub> absorption efficiency increased with temperature, liquid flow rate, and amine concentration as per the literature. During the absorption work, the Taylor flow regime was maintained at the reactor inlet. CO<sub>2</sub> desorption of loaded amine solutions was investigated at different concentrations and temperatures up to 85°C. MDEA solution had the highest desorption efficiency, followed by AMP and the least desorption efficiency was that of MEA. Foaming experimental results showed that MEA had a larger foaming region compared to AMP. However, more foaming happened with AMP at higher gas and liquid flow rates. A plug flow mathematical reactor model was developed to simulate the MEA-CO<sub>2</sub> system. The model captured well the performance and trends of the studied system, however the absolute prediction deviated due to uncertainties in the used physical properties and mass transfer correlation. Selecting a solvent for chemical absorption depends on many more factors than these three studied parameters. Still, microreactor proves a valuable tool to generate experimental results under different conditions, with the least amount of consumables (less than 1 L solvents were used), in a fast manner, combined with a knowledge insight because of the uniqueness of the Taylor flow regime.

**Keywords:** microreactor, CO<sub>2</sub> capture, solvent screening, absorption, desorption, amine

## 1 INTRODUCTION

CO<sub>2</sub> emission is one of the main contributors to global warming and considered a major environmental challenge in the last few decades. The annual global CO<sub>2</sub> emission is estimated at more than 40 billion metric tons, 85% of them are resulting from the combustion of fossil fuels such as coal, liquid hydrocarbon, and natural gas (IPCC, 2014). Capturing CO<sub>2</sub> from different industrial processes is an urgent need that requires developing cost-effective CO<sub>2</sub> capture, utilization, and storage (CCUS) technologies. Multiple carbon-capturing technologies are available such as cryogenic distillation, adsorption, membrane separation, and physical and chemical absorption (Cheung et al., 2013; Maqsood et al., 2014; Liang et al., 2015; Venna and Carreon, 2015). Out of these, chemical absorption using amine-based solvent technology is considered the most preferred and matured route for CO<sub>2</sub> capturing especially for post-combustion applications (Liang et al., 2015; Nwaoha et al., 2016; Aghel et al., 2018). Amines-based solvents are well-known for their reversible reactions with CO<sub>2</sub>, which make them ideal for the separation of many CO<sub>2</sub>-containing gases, including flue gases. The most commercially used amine-based solvents are monoethanolamine (MEA), diethanol amine (DEA), and N-methyldiethanolamine (MDEA). Even though the amine-based technology has been adopted by many industries, the overall cost of capturing process is still high if considering the global deployment of this technology. This is mainly due to the high capital investment, high energy consumption needed for solvent regeneration, loss of solvent due to evaporation and degradation, and plant corrosion issues (Abu-Zahra et al., 2007). The conventional CO<sub>2</sub> capturing units such as bubble column, packed column, and plate column are limited by gas-liquid mass transfer rate that demands larger sizes of the absorber and desorber units, therefore a large recirculation rate of solvents. The desorption unit is more complex and energy-intensive compared to the absorption unit. The higher temperature needed during regeneration contributes up to 80% of the total energy needed in the entire CO<sub>2</sub> capture process. This is needed for the heat of vaporization, and heating the larger amount of circulating amines and water in the process (Tobiesen et al., 2005). Besides energy needed for regeneration and mass transfer limitations, the CO<sub>2</sub> absorption unit faces other operational challenges such as foaming. It can occur during the plant start-up and operation of both absorber and regenerator. The common reasons for foaming in the alkanolamine system are the high gas velocities, process contaminations present with the feed gas that includes dissolved or condensed hydrocarbons, organic acid, water-soluble surfactants, additives, or sludge deposits in gas contactors. Foaming in the amine system dramatically lead to a decrease in the alkanolamine-gas absorption efficiency and requires the reduction of the gas velocity and feed flow rate to the absorber. Mitigating actions to regain the efficiency of the amine system in the gas treating plant include introducing anti-foaming additives altering the operating condition or incorporating mechanical filtration. Several studies on the effect of foaming and foam stability on the type of alkanol amine, liquid hydrocarbon, and the degradation products are

available in the literature (Thitakamol and Veawab, 2008; Alhseinat et al., 2014; Sedransk Campbell et al., 2015). Current operational practices focus more on solving the problem of foaming rather than identifying the sources of foam and eliminating them. This is because the foaming phenomenon is complex and depends on many factors. That is why experimental studies on foaming will remain very essential to overcome the foaming challenge and worth exploring new laboratory devices to study foaming close to process conditions. All of the above-mentioned challenges triggered a growing interest in developing new types of equipment with highly efficient absorber-desorber units to achieve process intensification (Wang et al., 2015). Among the different challenges associated with these technologies, solvent selection with the appropriate kinetic and mass transfer models is essential to deciding and optimizing the type of reactor technology and its optimal operating window.

Microreactor is an evolving technology with many achievements in a wide range of applications, especially in the laboratory and exploration stage (Mason et al., 2007; Hessel et al., 2008; Hartman and Jensen, 2009; Wirth, 2013; Yao et al., 2021). The basic concept of a microreactor is that reactants flow through a channel that has a characteristic diameter of micrometers to less than a few millimeters. As a result, the mixing and heating rates significantly increased due to the reduced diffusion length, and the increased surface to volume ratio. This enables a very precise and fast temperature control of the reaction environment as needed by the application. This makes the system very safe even for highly exothermic reactions. Besides, the mixing rate is well controlled and back mixing is significantly reduced. This is a major advantage compared to batch reactor systems which require new loading/unloading and cleaning when testing each condition. Also, the amount of required raw materials and waste produced are significantly reduced due to the small reaction channel volume. Another key advantage of microreactor is that it is an ideal venue for exploring the advantages of data science and artificial intelligence as demonstrated for a wide range of applications (McMullen and Jensen, 2010a; McMullen and Jensen, 2010b; Ganapathy et al., 2016; Reizman and Jensen, 2016).

Flowing a gas-liquid system in a microreactor results in different flow regimes such as bubbly, Taylor, churn, or annular flow. The choice of the flow regime depends on the gas and liquid flow rates, fluids' physical properties such as density, viscosity, surface tension, inlet mixer design, and the internal geometrical dimensions of the reactor. All of these flow regimes can be observed in a microreactor (Gupta et al., 2010). The small channel diameter confines the gas bubble and stabilizes the gas-liquid interface which is a major advantage compared to larger tube diameters (larger than 4 mm). Depending on the microreactor design, precise control of the gas bubble size and its movement can be realized. This is a key advantage when doing laboratory testing that requires a controlled environment. Of the different flow regimes, Taylor flow is a very promising one (Gupta et al., 2010; Al-Rawashdeh et al., 2012; Abiev et al., 2019; Abiev, 2020). **Figure 1**, shows a schematic example of this regime in a microreactor and its key definitions (Shao et al., 2009). The first advantage of Taylor flow is that the gas-liquid interface is well defined. Quantifying it is essential for

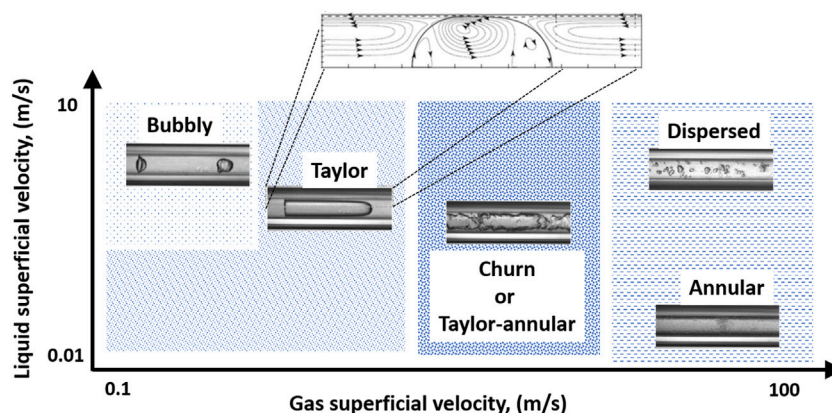


**FIGURE 1** | Flow patterns for gas-liquid flow depending on the gas and liquid flow rates. The modified image is adapted from Shao et al., 2009.

developing reliable mathematical models and engineering correlations. Second, each liquid droplet is well separated from the upstream ones, with less interaction between them that minimizes the back mixing approaching that of an ideal plug flow reactor. Third, the confined and moving liquid slugs and gas bubbles create secondary circular velocity profiles inside them. This helps accelerate further the rate of mass and heat transfer making this flow regime ideal for studying those applications with very fast reaction kinetics that are mass transfer limited such as the absorption-based CO<sub>2</sub> capturing (Cantu-Perez et al., 2013; Ganapathy et al., 2013; Bangerth et al., 2014; Sobieszuk et al., 2014; Yao et al., 2017; Aghel et al., 2019).

It is of great importance to have experimental laboratory tools that enable fast screening of conditions and solvents and link them to their industrial operation challenges. For the first time, foaming in combination with absorption and desorption studies is carried out in a microreactor setup for CO<sub>2</sub> capturing process. To the author's best knowledge, no reported work on foaming of CO<sub>2</sub> absorption coupled with a microreactor unit is reported in the open literature. Besides, most reported work on microreactor with CO<sub>2</sub> capturing deals with absorption only addressing the mass transfer performance challenge. A limited number of studies for CO<sub>2</sub> regeneration using microreactors are reported. To demonstrate the microreactor capabilities for absorption-desorption and foaming studies all in one go, three known amine-based solvents monoethanolamine (MEA), N-methyldiethanolamine (MDEA), and 2-amino-2-methyl-1-propanol (AMP) are selected for this work. Parametric studies are carried out by varying the amine solution flow rates, concentration, and reaction temperature. The tendency for foaming is evaluated in a gravity separator coupled to the microreactor system at different flow rates, and solvent concentrations. Throughout the entire work, gas-liquid Taylor flow is maintained at the reactor inlet and pure CO<sub>2</sub> is used to eliminate the gas phase mass transfer limitations and focus on the solvent screening. A mathematical reactor model is developed and the MEA absorption performance is evaluated. The model is used to assess the available mass transfer correlations to predict

the generated experimental results and link the work to other studies, conditions, and reactor types.

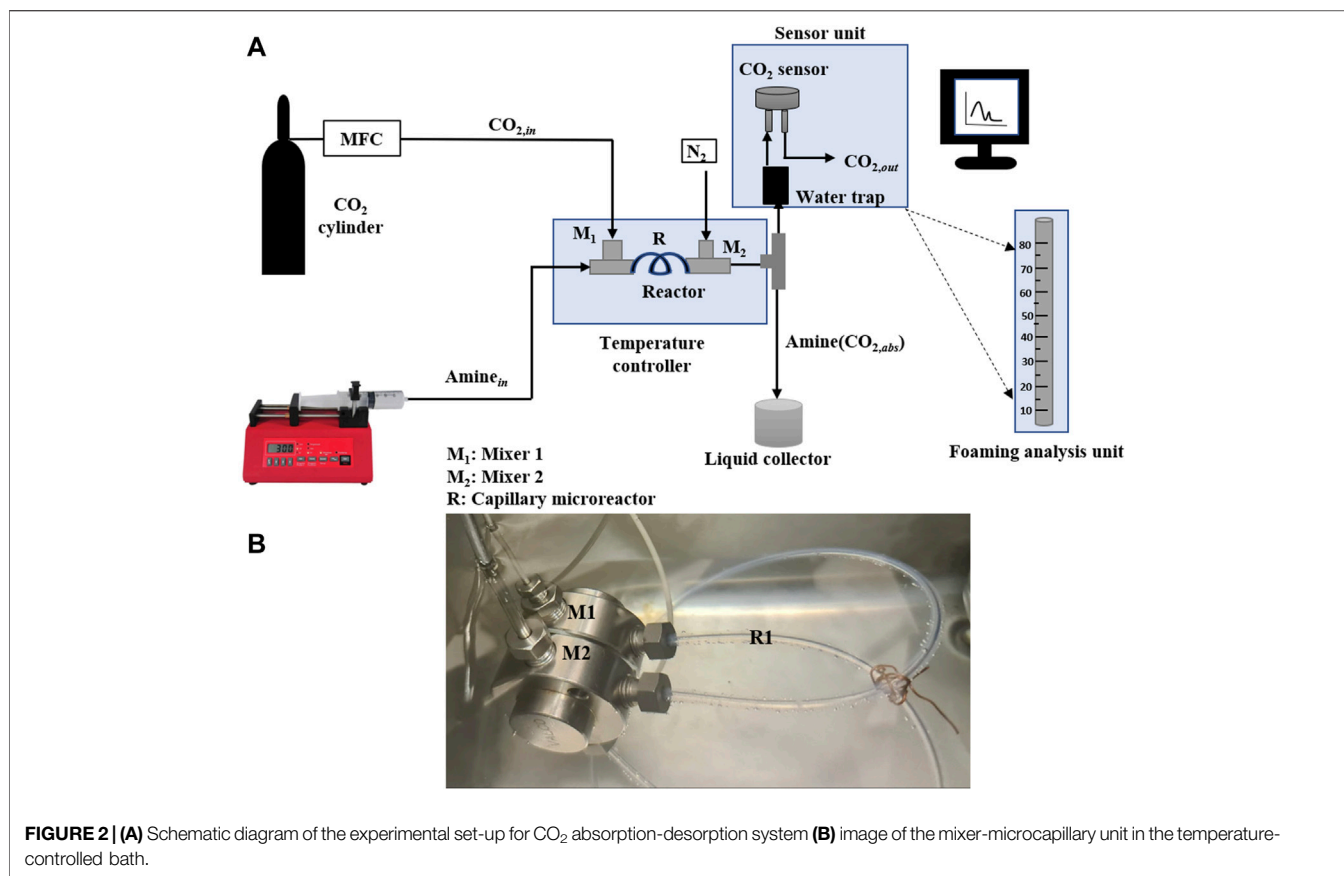
## 2 MATERIALS AND METHODS

### 2.1 Chemicals

Reagent grades of MEA (>98%), MDEA (>99%), and AMP (>90%) were obtained from Sigma-Aldrich, United States, and used without further purification. Aqueous solutions of MEA and MDEA were prepared at 6%, 12%, and 30 wt.% by dissolving the appropriate amount of amine in the deionized water at room temperature, while the aqueous solution of AMP was prepared by melting anhydrous AMP at 40°C and getting it dissolved in deionized water with the corresponding mass fraction. CO<sub>2</sub> (99.99%) gas used for the experiments was obtained from Buzwair Industrial Gases, Qatar. De-ionised water was used to prepare all solutions.

### 2.2 Experimental Setup

The experimental setup used in this work is shown in **Figure 2**. It consists of a programmable syringe pump (KF Technology) and the mass flow controller (Bronkhorst) that control the flow rate of the amine solution and CO<sub>2</sub> gas respectively. T-mixer (1/8" OD) was used to mix the gas and liquid streams and polymeric tubing (FEB with ID-0.060" OD-0.125") of 50 cm length was used as the capillary microreactor as shown in **Figure 2B**. The capillary microreactor and T-mixers were immersed inside a thermoregulated bath (Huber) filled with DI water to maintain the temperature of the system as needed and up to 85°C. The unabsorbed CO<sub>2</sub> was measured using a CO<sub>2</sub> sensor (CO<sub>2</sub> meter) placed at the outlet of the system. Readings from the CO<sub>2</sub> sensor were continuously recorded on a PC using a data acquisition system to measure the amount of CO<sub>2</sub> absorbed by the aqueous amine solution. Liquid samples of CO<sub>2</sub>-loaded amine solutions were collected from the amine liquid container to perform the desorption studies. The foaming studies were conducted using the same experimental set-up, however, the CO<sub>2</sub> sensor unit box was replaced by the foaming measuring device as shown in **Figure 2**.



The foaming analysis consists of a long marked tube to measure the height of height reached by the foam before it collapsed.

## 2.3 Procedure

At the start, different gas and liquid flow rates were varied to select the values needed to operate in the Taylor flow regime. It was decided to maintain the CO<sub>2</sub> gas flow rates at 6 and 9 ml/min for all absorption experiments. For each gas flow rate, the liquid flow rate was adjusted from a minimum value to a maximum value in such a way that the Taylor flow regime was maintained at the reactor inlet, and the CO<sub>2</sub> absorption efficiency varied from 0% to 100%. For each CO<sub>2</sub> absorption experiment, 30 ml of the desired amine solution (MEA, MDEA or AMP) was loaded into the syringe pump container. Pure CO<sub>2</sub> gas was added from a gas cylinder and regulated using Bronkhorst mass flow controller. The amine solution from the syringe (Amine<sub>in</sub>) and the CO<sub>2</sub> from the inlet side (CO<sub>2, in</sub>) were mixed in mixer M1 and then passed to the capillary microreactor. At the exit of the reactor, the loaded amine solution was mixed with a high nitrogen flow rate in the mixer M2 to minimize further absorption and quickly reach the CO<sub>2</sub> sensor. The reactor outlet goes after that to a gravity separator in which the CO<sub>2</sub>-loaded amines [Amine (CO<sub>2, abs</sub>)] are collected in the liquid container, and the unreacted CO<sub>2</sub> (CO<sub>2, out</sub>) will be detected by the CO<sub>2</sub> sensor and further passed to the vent. Before each experiment, calibration experiments are carried out to relate the CO<sub>2</sub> sensor measurement to the CO<sub>2</sub>

concentration in the effluent stream. All absorption experiments were conducted at atmospheric pressure and three different temperatures of 30, 40, and 50°C.

The absorption efficiency is calculated as shown in Eq. 1 by dividing the amount of CO<sub>2</sub> absorbed (CO<sub>2, abs</sub>) by the amount of inlet CO<sub>2</sub>.

$$\text{CO}_2\text{absorption efficiency} = \frac{(\text{CO}_{2, in} - \text{CO}_{2, out})}{\text{CO}_{2, in}} \quad (1)$$

Before starting the desorption analysis, the loaded CO<sub>2</sub> amine solution is prepared by carrying out an absorption experiment at given flow conditions with known CO<sub>2</sub> absorption efficiency. A sufficient amount of the CO<sub>2</sub>-loaded amine solution was collected in the liquid container and quickly loaded into the syringe pump. The CO<sub>2</sub>-rich amine solution was pumped through the capillary microreactor at different temperatures ranging from 50 to 85°C, and residence times by varying the liquid flow rate of the amine (Q<sub>L</sub>) from 0.1 to 1.2 ml/min. A small amount of nitrogen was added to the reactor to establish a gas-liquid interface for the desorption study. The desorption efficiency was measured using the CO<sub>2</sub> gas sensor and Eqs 2–4. Eq. 2 is used to calculate the amount of loaded CO<sub>2</sub> per amine flow rate in the absorption experiment. Then, the maximum amount of CO<sub>2</sub> that can be regenerated (max.CO<sub>2</sub> for regeneration) is calculated by multiplying the CO<sub>2</sub> loading obtained from Eq. 2 with the amine molar flow rate used during regeneration ( $F_{\text{Amine, reg}}$ ) as

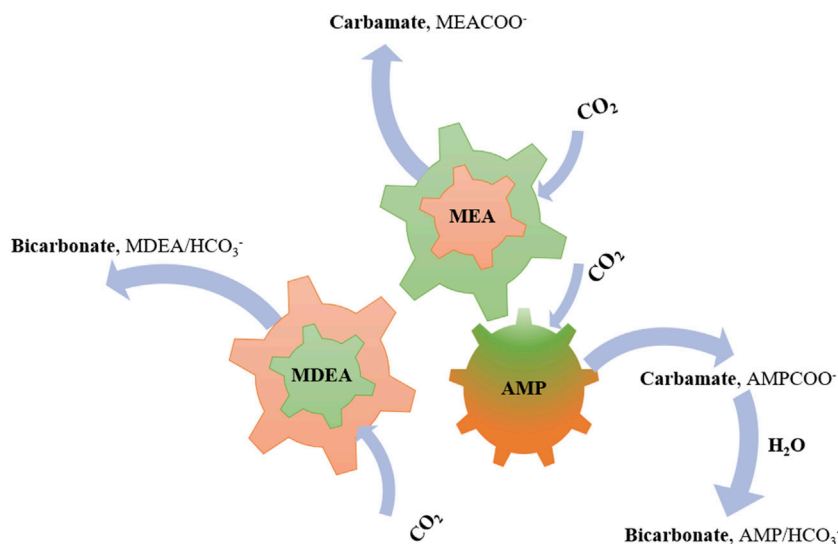


**FIGURE 3** | Typical reaction pathways of MEA, MDEA and AMP aqueous amine solutions.

shown in Eq. 3. Eq. 4 presents how the desorption efficiency is calculated by dividing the measured CO<sub>2</sub> molar flow rate by the maximum amount of CO<sub>2</sub> molar flow rate that can be regenerated.

$$\text{CO}_2 \text{ loading} = \frac{(F_{\text{CO}_2, \text{in}} - F_{\text{CO}_2, \text{out}})}{F_{\text{Amine}}} \quad (2)$$

$$\text{max. CO}_2 \text{ for regeneration} = \text{CO}_2 \text{ loading} \times F_{\text{Amine, reg}} \quad (3)$$

$$\text{Desorption efficiency} = \frac{F_{\text{CO}_2, \text{reg}}}{\text{max. CO}_2 \text{ for regeneration}} \quad (4)$$

The residence time ( $\tau$ ) was calculated using the below equation

$$\tau \text{ (sec)} = \frac{V_R \text{ (cm}^3\text{)}}{Q_L + Q_G \text{ (cm}^3\text{s}^{-1}\text{)}} \quad (5)$$

where  $V_R$  be the volume of the reactor and  $Q_L$  and  $Q_G$  be the volumetric flow rate of liquid and gas respectively. The foaming study was conducted using the gas-liquid separator shown in Figure 2 connected to the gas-liquid separator. For given amine and CO<sub>2</sub> flow rates, the nitrogen flow rate was changed between 0 and 60 ml/min to increase the tendency for foam generation in the gas-liquid separator. For each condition, the maximum reached foam height in the graduated tube was measured. To avoid foaming in the absorption and desorption studies, a gas-liquid separator with a larger volume was used and the inside was filled with small size metallic open structure that helped break the foaming. The measurement accuracy of the obtained results from the above-mentioned experimental setup was estimated between 1% and 4% for CO<sub>2</sub> absorption efficiency (%). This was obtained after quantifying repeated experiments. This accuracy depends on the accuracy of the CO<sub>2</sub> sensor ( $\pm 300$  ppm), the concentration of the amine solution, accuracies of the gas and liquid flow rates.

**TABLE 1** | Mechanism of CO<sub>2</sub> capture in aqueous amine solution.

Eqn No.	Equation
6	$2\text{H}_2\text{O} \leftrightarrow \text{H}_3\text{O}^+ + \text{OH}^- (k_1)$
7	$\text{CO}_2 + 2\text{H}_2\text{O} \leftrightarrow \text{H}_3\text{O}^+ + \text{HCO}_3^- (k_2)$
8	$\text{HCO}_3^- + \text{H}_2\text{O} \leftrightarrow \text{H}_3\text{O}^+ + \text{CO}_3^{2-} (k_3)$
MEA solution	
9	$\text{MEA} + \text{H}^+ \leftrightarrow \text{MEA}\text{H}^+ (k_4)$
10	$\text{MEA}\text{H}^+ + \text{H}_2\text{O} \leftrightarrow \text{MEA} + \text{H}_3\text{O}^+ (k_5)$
11	$2\text{MEA} + \text{CO}_2 \leftrightarrow \text{MEACOO}^- + \text{MEA}\text{H}^+ (k_6)$
12	$\text{MEACOO}^- + \text{H}_2\text{O} \leftrightarrow \text{MEA} + \text{HCO}_3^- (k_7)$
MDEA solution	
13	$\text{MDEA} + \text{H}^+ \leftrightarrow \text{MDEA}\text{H}^+ (k_8)$
14	$\text{MDEA} + \text{CO}_2 + \text{H}_2\text{O} \leftrightarrow \text{MDEA}\text{H}^+ + \text{HCO}_3^- (k_9)$
AMP solution	
15	$\text{AMP} + \text{H}^+ \leftrightarrow \text{AMP}\text{H}^+ (k_{10})$
16	$\text{AMP}\text{H}^+ + \text{H}_2\text{O} \leftrightarrow \text{AMP} + \text{H}_3\text{O}^+ (k_{11})$
17	$2\text{AMP} + \text{CO}_2 \leftrightarrow \text{AMP}\text{COO}^- + \text{AMP}\text{H}^+ (k_{12})$
18	$\text{AMP}\text{COO}^- + \text{H}_2\text{O} \leftrightarrow \text{AMP} + \text{HCO}_3^- (k_{13})$

## 3 REACTION MECHANISM AND REACTOR MODEL

### 3.1 Reaction Mechanism

Figure 3 shows the CO<sub>2</sub> reaction mechanism with the amine compounds. The reaction involves several unstable and reversible reactions in the aqueous phase as described in Eqs 6–18 in Table 1. The ionization reaction in the presence of CO<sub>2</sub> can be described by Eqs 6–8. The CO<sub>2</sub> reaction with the primary amine MEA can be expressed by Eqs 9–11 which involve the MEA protonation, stable MEA

carbamate formation, and MEA carbamate hydrolysis. The dominant carbamate formation reaction in the MEA is limited with the theoretical loading to 0.5 mol CO<sub>2</sub>/mol MEA. If the loading exceeds 0.5 mol CO<sub>2</sub>, a certain amount of MEA carbamate undergoes hydrolysis and generates standalone bicarbonates. Typically, the extent of hydrolysis is low, and regenerated free MEA during hydrolysis reacts again with free CO<sub>2</sub>, and further absorption proceeds. Hence, the advantage of using MEA is the formation of bonded carbamate that enhances the rate of absorption. However, it also slows down the rate of desorption.

MDEA is a tertiary amine, that does not involve any direct reaction with CO<sub>2</sub> due to the lack of free proton in the nitrogen atom, while it increases the hydroxyl ion concentration that catalyzes the CO<sub>2</sub> hydration that leads to the formation of bicarbonate as described by Eqs 13–14. The theoretical absorption capacity of MDEA is 1 mol CO<sub>2</sub>/mol amine, however, the absorption rate is slow compared to other primary and secondary amines. The notable advantages of using MDEA are the fast desorption rate and the large absorption capacity owing to the presence of bicarbonate ions as the only CO<sub>2</sub>-absorbing species. AMP is a hindered type of amine, which possesses either the characteristic of primary or secondary amine with the formation of unstable carbamate species as an intermediate product (Eq. 17) that quickly hydrolyzes to bicarbonates (Eq. 18). The presence of bicarbonate species as the dominant product enhances the desorption rate compared to MEA, its absorption rate is also higher when compared to the tertiary amine owing to the formation of unstable carbamate as the intermediate species.

### 3.2 Reactor Model

A mathematical reactor model was established to analyze the obtained absorption experimental results and carry out sensitivity analysis on mass transfer correlations available in the literature. A one-dimension ideal plug flow reactor model is established on the Taylor flow regime. Isothermal and isobaric conditions are maintained in this work. The mass transfer takes place only in the available gas-liquid interface. Only CO<sub>2</sub> is assumed to exchange between the two phases. Along the reactor length, the gas bubble sizes and gas hold-up will become smaller due to the CO<sub>2</sub> absorption. For some cases that reached 100% absorption efficiency, the gas bubble vanished and the reactor outlet consisted of pure liquid. To reflect on these changes, the gas holdup and the bubble length changes are accounted for in this reactor model. Following are the mass balance equations for the liquid and gas sides of this reactor model:

$$\frac{dC_{i,L}}{dz} = \frac{1}{u_L} (j_i + r_i \epsilon_L) \quad (19)$$

$$\frac{dC_{i,G}}{dz} = -\frac{1}{u_G} j_i \quad (20)$$

The mass transfer  $j_i$  will only be for the CO<sub>2</sub> molecule calculated as:

$$j_{CO_2} = k_1 a (C_{CO_2,G} - C_{CO_2,L}) \quad (21)$$

$$C_{CO_2,G} = \frac{P}{H} \quad (22)$$

The CO<sub>2,G</sub> concentration in the liquid phase is calculated using the solubility in Eq. 22. Henery's coefficient (H) is required in Eq. 22 to account for the solubility of CO<sub>2</sub> in the amine solution. Since mass transfer is a critical parameter in the performance of CO<sub>2</sub> absorption, multiple correlations in the literature shown in Table 2 are evaluated to find the one that best fits the experimental results.

In most of these correlations, gas and liquid hold-ups ( $\epsilon_G, \epsilon_L$ ), and slug and bubble lengths ( $L_S, L_B$ ) are required to estimate the mass transfer coefficient. Liquid hold up is needed in the mass balance as shown in Eq. 19. Using the imaging technique, some of the liquid slug and gas bubble lengths ( $L_S, L_B$ ) were measured at the inlet and outlet of the reaction channel. It was not always possible to estimate the slug and bubble length. Thus, these measured ( $L_S, L_B$ ) data were used to select a reliable equation to estimate their lengths for all other flow conditions. After estimating the ( $L_S, L_B$ ) lengths, the hold-ups are estimated as shown in Eqs 23, 25.

$$\epsilon_G = \frac{L_B}{L_B + L_S} \quad (23)$$

$$\epsilon_L = 1 - \epsilon_G \quad (24)$$

The length of the unit cell was estimated by:

$$L_{UC} = L_B + L_S \quad (25)$$

Regarding the reaction rate for MEA, the widely accepted bimolecular kinetic law shown in Eq. 26 is used (Ramezani et al., 2019). Several estimates for the reaction rate constant can be found in the literature (Blauwhoff et al., 1983; Versteeg et al., 1996; Aboudheir et al., 2003). However, most of these works did not use microreactors when developing their kinetic model. The proposed Arrhenius equation developed by Ye et al. (2013) was used in this work because it has been validated in microreactor setup. The value of the rate constant  $k_1$  ( $m^3/mol s$ ) is shown in Eq. 27.

$$r_{CO_2} = k_1 C_{MEA} C_{CO_2,L} \quad (26)$$

$$k_1 = 1.09 \times 10^6 \exp\left(-\frac{2671.4}{T}\right) \quad (27)$$

## 4 RESULTS AND DISCUSSION

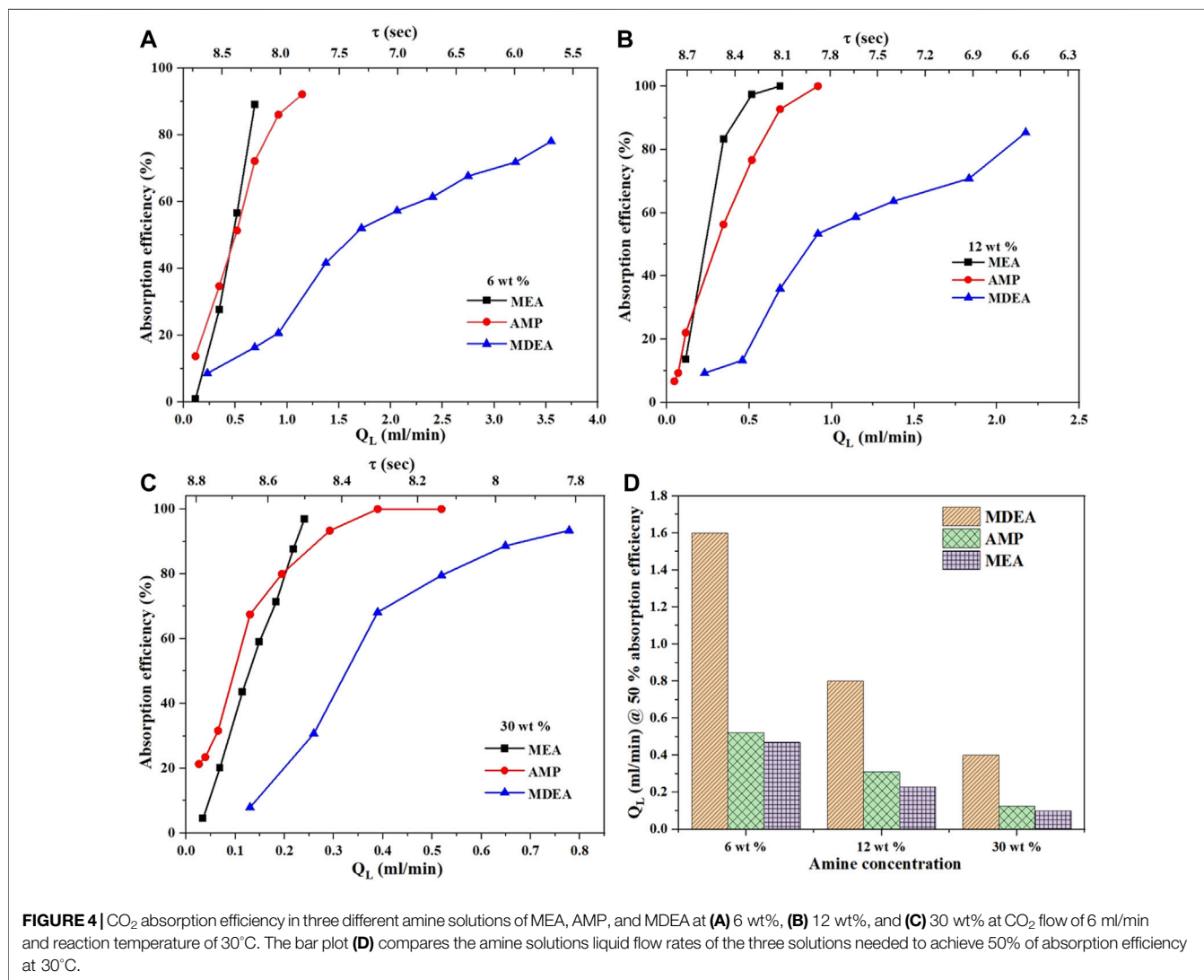
### 4.1 Absorption Studies on Aqueous Amines

#### 4.1.1 Effect of Amine Solvents Type and Concentration

The screening of three different amine solutions in terms of CO<sub>2</sub> absorption efficiency at different liquid flow rates and concentrations is shown in Figure 4. All these experiments were conducted at a fixed CO<sub>2</sub> gas flow rate of 6 ml/min and a constant temperature of 30°C. The absorption efficiency increases the amine flow rate  $Q_L$ . Increasing the flow rate decreases the gas bubble length which increases the specific interfacial area, thus increasing the rate of mass transfer. As

**TABLE 2** | List of liquid volumetric mass transfer coefficients for Taylor flow regime in a microreactor.

References	Index	Correlation	Description
Berčić and Pintar, (1997)	lka1	$k_L a = \frac{0.111(u_B + u_L)^{1.19}}{((1-\epsilon_0)L_{UC})^{0.57}}$	d = 1.5; 2.0; 3.1 mm (Circular)
Vandu et al. (2005)	lka2	$k_L a = 4.5 \sqrt{\frac{Du_B}{L_{UC}}} \frac{1}{d_h}$	d = 1.0; 2.0; 3.0 mm (Circular)
Yue et al. (2007)	lka3	$k_L a = \frac{(\frac{1}{9}0.084Re_G^{0.213}Re_L^{0.937}Sc_L^{0.5})D}{d}$	d = 0.667 mm (Circular)
Yue et al. (2009)	lka4	$k_L a = \frac{2}{d_h} \sqrt{\frac{Du_B}{L_B + L_S}} \left(\frac{L_B}{L_B + L_S}\right)^{0.3}$	d <sub>h</sub> = 0.4 mm (Square); u <sub>B</sub> = 0.4–2.0 m/s; 1.4 ≤ L <sub>B</sub> /d ≤ 6.3; 1 ≤ L <sub>S</sub> /d ≤ 3.2
Lefortier et al. (2012)	lka6	$k_L a = 1.19 \sqrt{\frac{Du_B}{dL_S^2}} + 0.65 \frac{L_B}{L_S} \sqrt{\frac{Du_B}{d^2 L_B}}$	r = 91 μm (nearly half-circle)
Zhu et al. (2014)	lka7	$k_L a = 2 \frac{\sqrt{2}}{\pi} \sqrt{\frac{Du_B}{d}} \frac{4}{L_{UC}} + \frac{2}{\sqrt{\pi}} \sqrt{\frac{Du_B}{\epsilon_0 L_{UC}}} \frac{4\epsilon_0}{d}$	d = 1.5; 2.0; 3.0 mm (Circular); u <sub>B</sub> = 0.09–0.65 m/s; L <sub>UC</sub> = 5–60 mm
Abolhasani et al. (2015)	lka8	$k_L a = \frac{8}{L_{UC}} \sqrt{\frac{2Du_B}{\pi^2 d_h}}$	d <sub>h</sub> = 300 μm (Square)



well, the molar ratio between the amine and CO<sub>2</sub> increases which facilitates the reaction to proceed further. This trend is observed for all amine solutions at all concentrations. The lowest absorption efficiency was for MDEA followed by AMP then

MEA. This trend matches the literature as the reaction kinetics of tertiary amine MDEA is lower compared to those of MEA and AMP. Thus, a higher liquid flow rate will be required to achieve the same absorption efficiency. For some conditions,

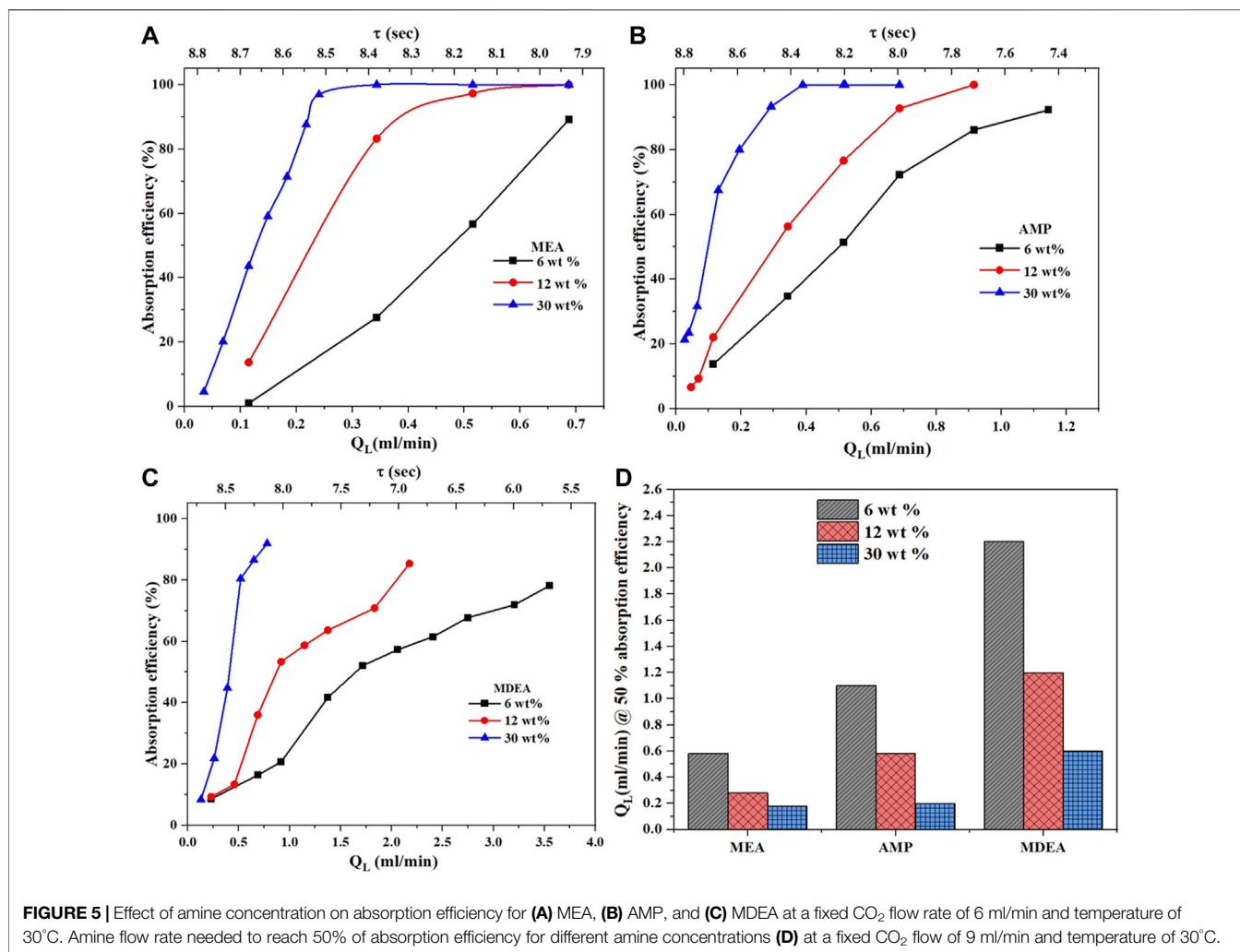


**FIGURE 5 |** Effect of amine concentration on absorption efficiency for (A) MEA, (B) AMP, and (C) MDEA at a fixed CO<sub>2</sub> flow rate of 6 ml/min and temperature of 30°C. Amine flow rate needed to reach 50% of absorption efficiency for different amine concentrations (D) at a fixed CO<sub>2</sub> flow of 9 ml/min and temperature of 30°C.

the absorption rate changes between MEA and AMP depending on the used liquid flow rates. For example, at  $Q_L < 0.45$  ml/min in **Figure 4A**, the absorption efficiency for AMP is slightly higher than that of MEA. However, this trend flipped when the liquid flow rate increased. This flip can not be explained solely by the molarity difference between AMP and MEA. Other factors such as viscosity, solubility, and diffusivity can have a significant contribution to absorption efficiency.

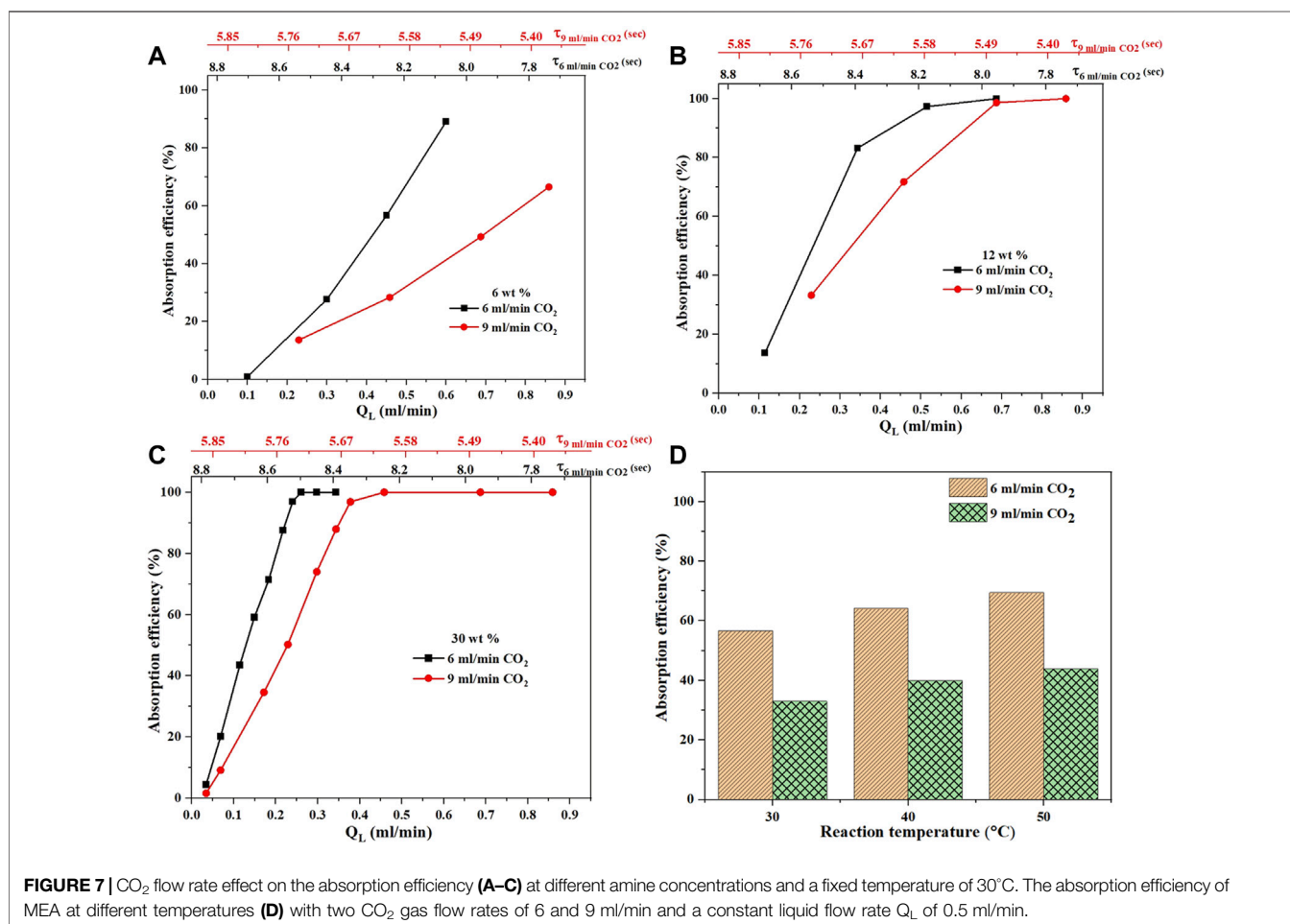
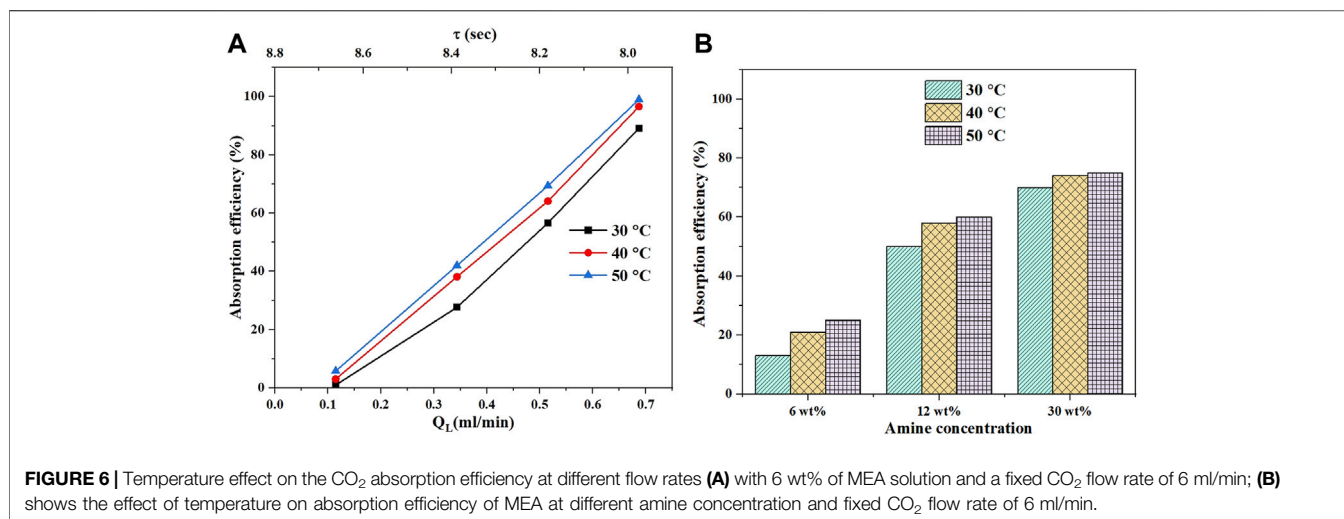
For the sake of clarity, the absorption efficiency per amine type is shown in **Figure 5**. In all cases, the absorption efficiency increases with concentration because of the increase in the molar ratio between the amine and used CO<sub>2</sub>. For MEA, a linear relation for the three different concentrations is observed. For AMP, this is not the case and deviation from a linear relationship is observed. As the AMP concentration increases, this deviation increases. Increasing the concentration will affect the physical properties of diffusion, solubility, and viscosity which can change differently for each solvent and concentration which could be the reason for this observation. For MDEA, a pseudo-linear trend is observed between the absorption efficiency and liquid flow rate. As the

concentration increases, the absorption efficiency increases but is less than that for AMP and MEA.

**Figure 4D** shows the comparison of MDEA, AMP, and MEA at different amine concentrations and the corresponding  $Q_L$  values to achieve 50% absorption efficiency. MDEA requires a much higher liquid flow rate, followed by AMP, and then MEA. A similar trend is observed in **Figure 5D** for different amine concentrations at a fixed CO<sub>2</sub> flow of 9 ml/min and a temperature of 30°C. Overall, the most promising solution to use in terms of absorption efficiency is that of the primary MEA aqueous solution, followed by AMP, then MDEA. The higher the amine concentration, the faster the rate of absorption. All the trends in this section match the literature which demonstrates the capability of the microreactor setup to screen solvents for CO<sub>2</sub> absorption efficiency.

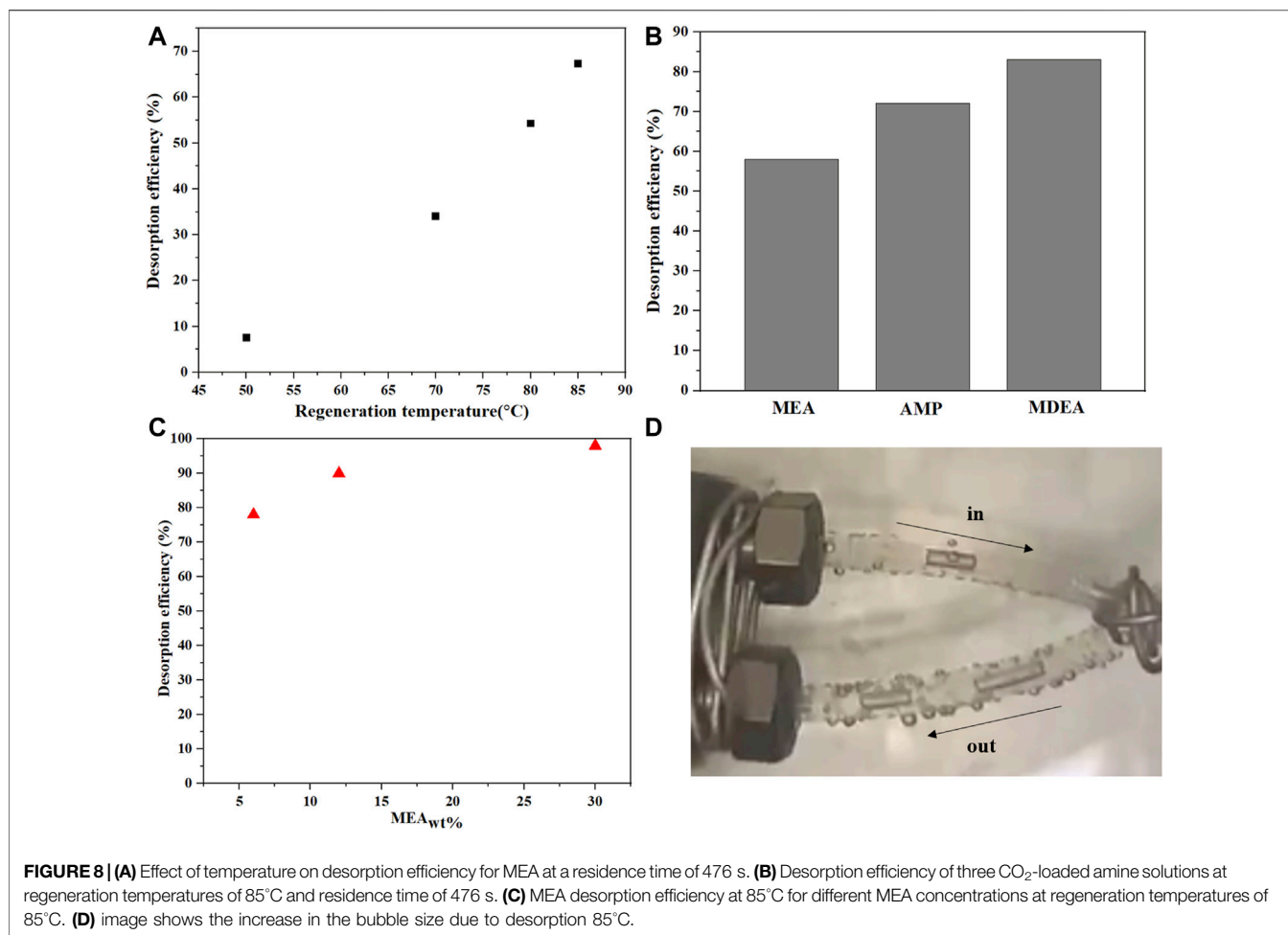
#### 4.1.2 Effect of Temperature Using Monoethanolamine

This section evaluates the absorption efficiency at different temperatures for MEA only. **Figure 6A** shows the effect of temperature change from 30 to 50°C on the CO<sub>2</sub> absorption efficiency using 6 wt% MEA at a fixed CO<sub>2</sub> flow rate of 6 ml/min



and different liquid flow rates. As the temperature increases, the absorption efficiency increases. However, the rate of increase from 40 to 50 °C is less when compared with that from 30 to 40 °C. The increase in temperature causes an increase in reaction rate constant and accelerates the chemical absorption. However, the

rate of desorption increases as well which limits the overall rate of absorption due to the thermodynamic limits of the reaction. Additionally, the increase in temperature will decrease the CO<sub>2</sub> solubility as ( $C_{CO_2,G} = \frac{p}{H}$ ) as Henry's coefficient (H) reduces with temperature. The viscosity of the amine solution reduces as



the temperature increases; however, the impact on mass transfer should not be that significant as compared to the other earlier mentioned parameters. Thus, there is an optimal operating temperature between 30 and 40°C that balances out the rate of absorption with the rate of desorption. The same conclusions are observed when the amine concentrations are adjusted as shown in **Figure 6B**. As the amine concentration increases, the difference in the absorption efficiency between the three different temperatures reduces. This is due to the different kinetics parameters of each amine in terms of rate constant and involved reaction mechanism.

#### 4.1.3 Effect of CO<sub>2</sub> Flow Rate Using Monoethanolamine

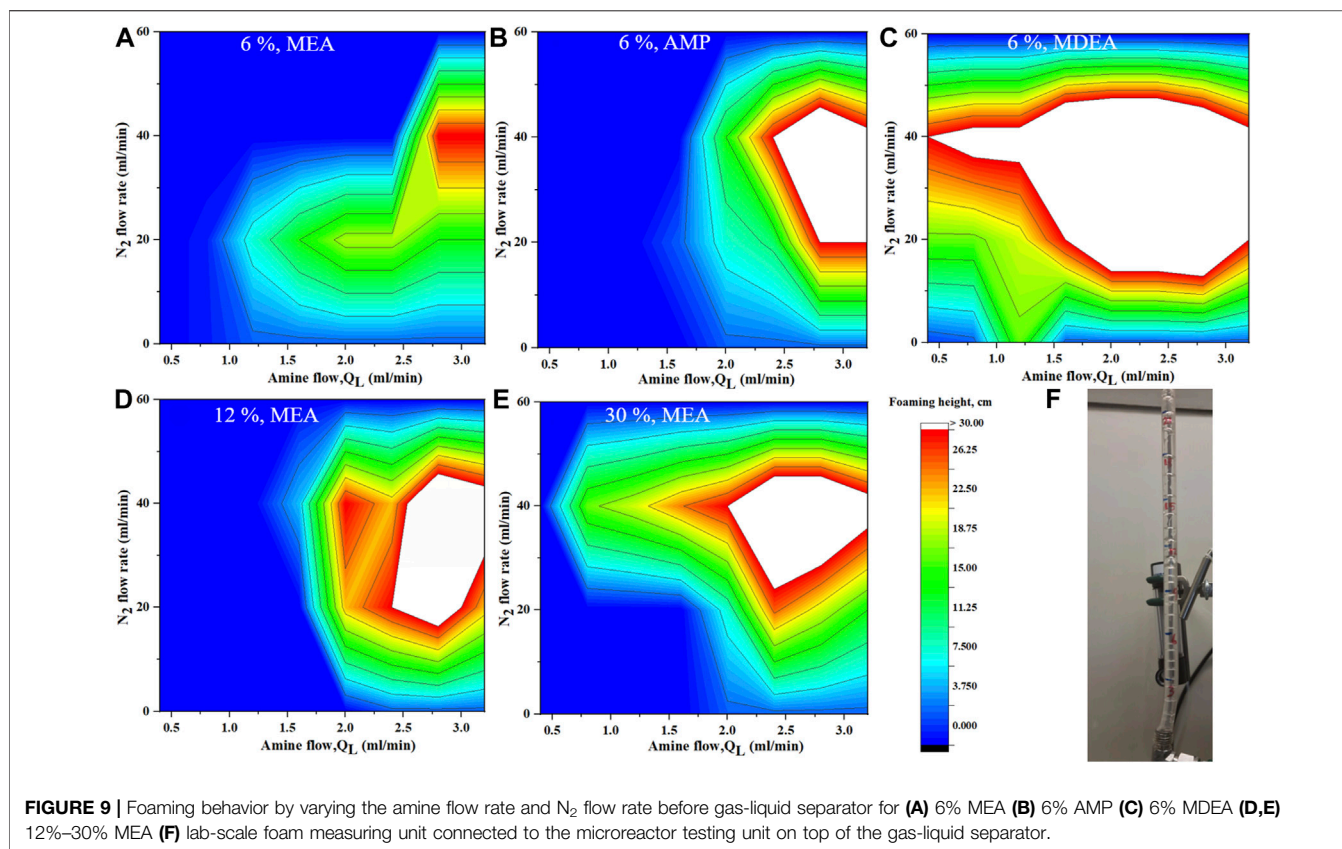
The effect of CO<sub>2</sub> gas flow rate on the absorption efficiency is demonstrated for MEA only as shown in **Figure 7**. For all the MEA concentrations, and flow rates, the absorption efficiency was higher for the 6 ml/min than that of the 9 ml/min CO<sub>2</sub> flow rate. Within the mentioned gas flow rates, the expected change in mass transfer coefficient should not be that significant. However, the available specific interfacial area will change thus affecting the rate of mass transfer. As the CO<sub>2</sub> gas flow rate increases, the gas bubble length increases which reduces the specific interfacial area.

The lower the interfacial area the lower the rate of absorption. Besides, as the gas flow rate increases, the residence time decreases which reduces the rate of absorption.

The trend of absorption efficiency is the same for all the different MEA concentrations and temperatures as shown in **Figure 7**. However, when the concentration changes the slope between the rate of absorption and liquid flow rates changes. According to Zwitterion mechanism (Caplow, 1968), as the MEA concentration increases, the reaction order changes from one to two which explains why the slopes become much steeper at higher MEA concentrations. For both CO<sub>2</sub> flow rates, the absorption efficiency changes with temperature in a similar manner as explained earlier in **Section 4.1.2**. The presented results show how sensitive is the rate of CO<sub>2</sub> absorption to the amine concentration, temperature, and flow rates. The fine balance between these parameters and the optimal conditions that maximize the rate of CO<sub>2</sub> can only be done with the help of a mathematical reactor model.

## 4.2 Desorption Studies

This section evaluate the desorption efficiency or regeneration at different conditions demonstrated using MEA solvent only. **Figure 8** shows the desorption efficiency for CO<sub>2</sub>-loaded MEA



at a given flow rate (residence time corresponding to 479 s) and different regeneration temperatures. This residence time was chosen in such a way that sufficient desorption is obtained to allow a fair analysis of the solvent behavior for different regeneration temperatures while maintaining isothermal conditions in the reactor tube. As the temperature increases, the desorption rate increases as shown in **Figure 8A**. Apart from the study at 50°C, The desorption efficiency exhibited a linear relation with applied temperature. This demonstrates the capability of the microreactor to facilitate the gas desorption from the heated liquid owing to the high surface-to-volume ratio. At 50°C, the rate of absorption is still significant compared to desorption as explained earlier in **Section 4.1.2**. That is why desorption efficiency at this temperature deviates from the other high temperatures. **Figure 8B** shows a comparison between three CO<sub>2</sub>-loaded amine solutions in terms of desorption efficiency at a temperature of 85°C. The highest desorption efficiency was observed for MDEA, followed by that of AMP and the last was that of MEA. This trend matches the data reported in the literature (Aghel et al., 2020). MDEA has the highest desorption rate owing to the presence of bicarbonate ions as the only CO<sub>2</sub> absorbing species the opposite of MEA which holds the lowest desorption rate during regeneration due to the stable carbamate bonds that require more energy to break down. The desorption efficiency of MEA is 1.5 times lower than MDEA at a regeneration temperature of 85°C.

**Figure 8C** shows the MEA desorption efficiency at 85°C for different MEA concentrations. The desorption efficiency is higher for 30 wt% and decreases as the MEA concentration decreases. With increased amine concentration, more CO<sub>2</sub> is available and chemically bonded to MEA. Hence, more CO<sub>2</sub> is expected to be released at a given temperature. In all desorption studies, a small amount of nitrogen was added to the reactor to establish a gas-liquid interface for the desorption study. Without this gas-liquid interface, gaseous molecules need to be first created before the gas bubble can grow due to the CO<sub>2</sub> regeneration reaction. To avoid the complexity associated with the gas phase formation, the gas-liquid interface was created before desorption started to take place. In all of the desorption experiments a small amount of N<sub>2</sub> was added in the inlet to create a gas-liquid interphase which helped the reaction to proceed more smoothly and to avoid the complexity associated with the gas phase formation/nucleation as the experiments was only carried out at 85°C. Without this gas-liquid interface, gaseous molecules need to be first created before the gas bubble can grow due to the CO<sub>2</sub> regeneration reaction. This is limited at the temperature condition of 85°C used in this work. **Figure 8D** shows how the gas bubble size increases in the capillary microreactor due to desorption at 85°C, which confirms the desorption of CO<sub>2</sub> from the amine solution.

### 4.3 Foaming Analysis

A study on the foam formation at different amine solutions is shown in **Figure 9** for different liquid and nitrogen flow rates

added before the gas-liquid separator. For all the studies, the foaming increases when the gas and liquid flow rates increase matching the literature data. The increase in foaming is not linear but reaches a maximum at intermediate regions of gas and liquid flow rates. For example, in the case of 6 wt% MEA and a fixed liquid flow rate of 1.5 ml/min, the foaming at a low N<sub>2</sub> gas flow rate is minimal and starts to increase with increasing the flow rate reaching maximum foaming at 20 ml/min. Increasing the N<sub>2</sub> gas flow rate beyond that reduces the foaming. This is because the created turbulence will increase which disrupts the foam formation and reduces its stability. A similar analysis can be carried out for a fixed gas flow rate. For example, at a fixed N<sub>2</sub> gas flow rate of 40 ml/min, no foaming existed when the liquid flow rate was below 2.5 ml/min. This means the hydrostatic force is inadequate to resist the buoyancy force of the N<sub>2</sub> bubble. Once the liquid flow rate increases to more than 2.5 ml/min, foams are produced and increased with the liquid flow rate. The increase in liquid flow rate leads to an increase in the hydrostatic force which in turn reduces the turbulence caused by the bubble detachment from the diffuser. As the liquid flow rate further increased, foaming became invariant. The increasing hydrostatic force overcomes the turbulence caused by the bubble detachment or makes such turbulence insignificant (Thitakamol et al., 2009).

When the MEA concentration increased from 6 wt%, to 12 wt % to 30 wt%, the region of foaming became wider with some variations in the foaming height. As the MEA concentration increases, the surface tension of the solution decreases while the density and viscosity increase. The bulk viscosity plays a significant role in the rising bubbles through the liquid phase to form a foam layer as explained by the creaming process. The decrease in foaming formation is caused by a reduction in the foam stability due to an increase in the surface viscosity of the solution (Thitakamol et al., 2009).

The foaming tendency of selected amines was evaluated as shown in **Figure 9**. Overall, the MDEA showed the highest tendency for foaming followed by MEA and finally AMP. Although the region of foaming for AMP was less, the height of foaming was more than that of MEA. In general physical properties, particularly surface tension, density, and viscosity, play a determinant role in foaming formation and stability. These properties should be considered in any study or strategy for foaming development and control in the future. MDEA in this experiment was the worst foaming, which is not matching the literature. Since foaming is a complex phenomenon and can be affected by many other factors, further investigations are needed to better confirm the foaming result under wider conditions, for different concentrations, and thermally degraded amine to have more clarity results.

#### 4.4 CO<sub>2</sub>-Monoethanolamine Reactor Model

The earlier presented results show how sensitive is the rate of CO<sub>2</sub> absorption to the amine concentration, temperature, and flow rates which affect the kinetics and rate of mass transfer. The fine balance between these parameters and maximizing the CO<sub>2</sub> capturing rate can only be done with the help of a mathematical reactor model. Using MEA as an example, a

mathematical reactor model is developed (see **Section 3.2**) and used to simulate all the generated experimental data based on available correlations from the literature. Initially, the model failed to provide an adequate prediction of the experimental results. Sensitivity analysis indicated that the liquid hold-up (used in **Eq. 19**) significantly affected the model prediction. The liquid hold-up is estimated based on the slug and bubble lengths as shown in **Eq. 23**. In this work, some measurements of the gas bubble and liquid slug lengths were done, but for some conditions such as high temperatures, and low liquid flow rates, this was not feasible. As well, the slug and bubble lengths fluctuated to a certain degree which introduce a level of inaccuracy in their measurement. Thus, the best approach was to use a mathematical correlation to predict the average gas and liquid slug length and have this correlation validated on those measured slugs and bubble lengths. Different correlations from the literature were evaluated in this work. The correlations that best predicted the available slug and bubble length measurements were the ones generated by (Haase et al., 2016) as shown in **Eqs 28, 29**. These correlations were selected and used in all further work.

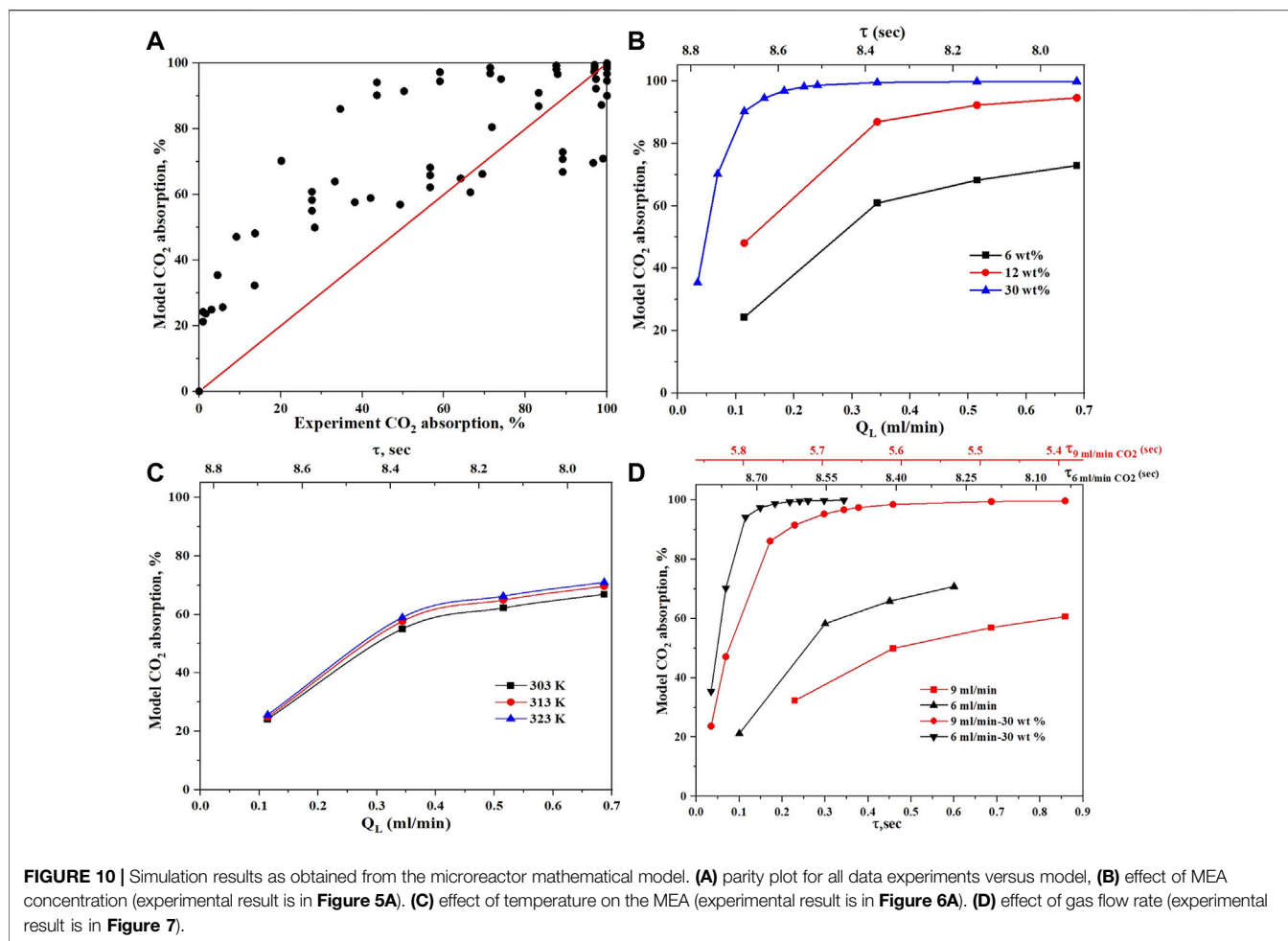
$$L_B = \left(1 + 0.57 \frac{u_G}{u_L}\right) d_h \quad (28)$$

$$L_S = \frac{\left(1 + 0.57 \frac{u_G}{u_L}\right) d_h (1 - \beta_G)}{\beta_G} \quad (29)$$

The next model parameter that affected the reactor model prediction was the volumetric mass transfer coefficient used in **Eq. 21**. Eight different correlations from the literature as shown in **Table 2** were evaluated. The correlation that best predicted the experimental data was the second correlation Ik2 by (Vandu et al., 2005). At this stage, the model prediction improved significantly and managed to capture all the trends of the experimental results correctly. However, lower prediction accuracy especially at high or low conversions was observed, at the same time the model was not sensitive to the amine concentration or temperature effect. This can be explained by the fact that all simulation works at this stage were performed assuming constant physical and transport properties. The effect of the temperature and the amine concentration on the viscosity, diffusivity, and solubility of CO<sub>2</sub> was not considered which was found to have a significant impact on the model prediction. To account for these effects, Henry's coefficient was taken from the work of (Li et al., 2017), and the viscosity was estimated from the work of (Arachchige et al., 2013). The diffusion coefficient of CO<sub>2</sub> in MEA ( $D_{CO_2,MEA}$ ) was estimated using the N<sub>2</sub>O analogy which requires three known parameters to calculate the unknown fourth parameter ( $D_{CO_2,MEA}$ ) as shown in **Eq. 30**.

$$\frac{D_{CO_2,MEA}}{D_{N_2O,MEA}} = \frac{D_{CO_2,H_2O}}{D_{N_2O,H_2O}} \quad (30)$$

Using **Eqs 31, 32**, the diffusion coefficients of CO<sub>2</sub> and N<sub>2</sub>O in water (H<sub>2</sub>O) were calculated (Versteeg et al., 1987; Versteeg and van Swaal, 1988).



$$D_{CO_2,H_2O} = 2.35 \times 10^{-6} \exp\left(-\frac{2119}{T}\right) \quad (31)$$

$$D_{N_2O,H_2O} = 5.07 \times 10^{-6} \exp\left(-\frac{2371}{T}\right) \quad (32)$$

to calculate the diffusion coefficient of N<sub>2</sub>O in MEA ( $D_{N_2O,MEA}$ ), **Eq. 33** was used. In this case, the diffusion coefficient of N<sub>2</sub>O in MEA was related to the diffusion coefficient of N<sub>2</sub>O in water and the viscosities of MEA and Water respectively. The coefficient Gamma ( $\gamma$ ) was taken to be equal to 0.51 for MEA. The dynamic viscosity estimation as a function of temperature from the work of (Korson et al., 1969; Sada et al., 1978).

$$D_{N_2O,MEA} \times \mu_{MEA}^{\gamma} = D_{N_2O,H_2O} \times \mu_{H_2O}^{\gamma} \quad (33)$$

After accounting for the non-constant physical and transport properties in the reactor model, the predictions became more reasonable as shown in **Figure 10**. The effect of MEA concentration was predicted well as shown in **Figure 10B** which matches the experimental results in **Figure 5A**. The effect of temperature on the MEA absorption is shown in **Figure 10C**, which matches the experiments in **Figure 6A**. The effect of gas flow rate is also shown in **Figure 10D** and matches the experimental results in

**TABLE 3** | Qualitative performance of amine solutions screening the capillary microreactor setup.

Phenomena	Absorption	Desorption	Foaming
Amine solution			
MEA	best	worst	average
AMP	average	average	average
MDEA	worst	best	worst

**Figure 7**. Overall, the mathematical reactor model was good enough to provide a reasonable prediction for the experimental results, however, further, and development to consider other solvents than MEA is still needed. This work demonstrates how critical the physical and transport properties such as diffusivity, Henry's coefficient, and viscosity are to the accuracy of the model prediction. For example, when evaluating the different mass transfer correlations presented in **Table 2**, the worst predictions were for the correlations that did not account for these physical properties inside them. For a given microreactor system, the model prediction can be significantly improved

**TABLE 4** | Selection criteria for liquid chemical absorbents.

Practical factors	Absorption performance	Desorption performance	Operational challenges	Physical properties
Cost	CO <sub>2</sub> loading capacity	Regeneration energy	Foaming	Viscosity
Toxicity	Absorption rate and CO <sub>2</sub> reactivity	Regeneration rate	Corrosivity	Surface tension
	Heat of absorption		Thermal stability	Vapour pressure

if a dedicated correlation for slug and bubble lengths is developed because these lengths are strongly controlled by the geometry and dimensions of the mixer and reactor channel.

#### 4.5 Solvent Selection and Perspective to Other Conditions and Reactors

Overall, the experimental setup and procedures developed in this work were able to perform an initial screening of different amine-based solvents. **Table 3** shows a qualitative judgment of the obtained results for three studied parts of absorption, desorption, and foaming. It is clear that a compromise is needed to define the optimal solvent. Selecting a solvent for chemical absorption depends on many more factors than what is studied in this work as shown in **Table 4** (Shokrollahi et al., 2022). It will require conducting a comprehensive assessment to address all these factors supported by techno-economic calculations that are beyond the scope of this work.

The developed theoretical reactor model was well linked to the experimental results. For a detailed assessment, the experimental setup needs to be adjusted to reflect industrial conditions. Some suggestions are proposed to enhance the experimental setup performance and the reactor model prediction. Installing an online gas-liquid separator rather than a gravity separator enables a more accurate prediction of the absorption and desorption results. Making a microreactor plate integrated with a heat exchanger, can be much more efficient to control the temperature and more practical to apply imaging techniques. Applying imaging techniques in a water bath to measure slug and bubble lengths was not feasible all the time, especially at high temperatures. Using integrated analytics to measure slug and bubble length can improve the estimation of the mass transfer correlation. Installing a back-pressure regulator can enable screening at higher pressure. Using a continuous liquid pump can enable continuous operation of the regenerated amine, thus screening the solvent with amines that have been exposed to thermal treatment. And finally analyzing the liquid samples will provide much more insight into the chemistry of the reaction and amine performance. Incorporating these features into the experimental setup can open new opportunities for faster and more efficient solvent screening in the future under more industrially relevant conditions.

Although microreactors outperform many industrial reactors when it comes to mass transfer limited reactions, it has limitations to be used at an industrial scale for application

as post-combustion CO<sub>2</sub> capturing. This is mainly due to the large pressure drop, chances of blockage, and the large capital cost of microreactors as they do not take advantage of the economy of scale. Current industrial reactors for CO<sub>2</sub> capturing will have much lower mass transfer rates and different gas-liquid hydrodynamics compared to the microreactors. Thus, can solvents that are screened in a microreactor be used in other types of industrial reactors? This requires experimental validation, but theoretically speaking, there are no foreseen reasons why not. The emphasis when using the laboratory microreactor is how the different amine solvents performed against each other. If the reactor type or conditions will change for all of the solvents in the same way, there is no reason why the solvent performance against each other will change.

## 5 CONCLUSION

This work uses a simple microreactor setup made of capillaries to screen and evaluate three types of amine-based solvents (MEA, MDEA, and AMP) at different conditions regarding absorption, desorption, and foaming. This is the first time that these three performances are combined in a microreactor setup and studied in one go. Known solvents were used to show the capability of this setup and the potential of using Taylor flow regime because of its well-defined flow regime and attractive features. A plug flow mathematical reactor model was used to simulate the CO<sub>2</sub> absorption performance for the CO<sub>2</sub>-MEA-H<sub>2</sub>O system. The performance and trends were well captured by the model to a certain degree. The absolute prediction however was not so good with an error reaching up to 50% for some conditions. This was mainly due to the poor estimation of the physical properties such as Henry's coefficient, diffusivity, and viscosity of the amine solutions when their concentrations and compositions were altered, as well as the correlation used for the mass transfer coefficient.

The CO<sub>2</sub> absorption and desorption efficiencies are highly influenced by various operating factors such as liquid-gas flow rate, reaction temperature, amine concentration, and the type of amine used in the microreactor. The highest CO<sub>2</sub> absorption efficiency was achieved at a smaller gas flow rate and a larger liquid flow rate. Higher temperature resulted in higher absorption efficiency, however, increasing it further increases the rate of desorption which confirmed the need for an optimum temperature. In the case of MEA, this optimum temperature was in the range of 30–40°C. MEA

has the highest absorption efficiency, followed by AMP, and then MDEA. However, MEA has the lowest desorption efficiency and MDEA has the highest one. Increasing the regeneration temperature, and amine concentrations increase the rate of desorption. Each amine solution follows its absorption kinetics as visible from the different absorption trends which are linked to the dominant reaction mechanism. The most noticeable changes were when the mole ratio between CO<sub>2</sub> and the available amine sites was altered. Considering the aspect of foaming, MEA had a larger region for foaming compared to AMP, but AMP foamed to a higher degree at higher gas and liquid flow rates. Since foaming is a complex phenomenon and can be affected by many other factors, further investigations are needed to better confirm the foaming result under wider conditions, for different concentrations, and thermally degraded amine to have more clarity results on the foaming.

Selecting a solvent for chemical absorption depends on many more factors than these three parameters of absorption, desorption, and foaming. A comprehensive assessment to address all these factors supported by techno-economic calculations will be needed. Microreactor can be one of the laboratory devices that can support this comprehensive assessment. Even with a relatively simple setup, many valuable experimental results were generated under different conditions, with the least amount of consumables (less than 1 L for all solvents), in a fast manner, and combined with a fundamental insight because of the uniqueness of the Taylor flow regime and reactor model. Suggestions are proposed to enhance the experimental setup performance and the reactor model. Incorporating these features can open new opportunities for faster and more efficient solvent screening in the future under more industrially relevant conditions.

## REFERENCES

- Abiev, R. S., Butler, C., Cid, E., Lalanne, B., and Billet, A.-M. (2019). Mass Transfer Characteristics and Concentration Field Evolution for Gas-Liquid Taylor Flow in Milli Channels. *Chem. Eng. Sci.* 207, 1331–1340. doi:10.1016/j.ces.2019.07.046
- Abiev, R. S. (2020). Gas-liquid and Gas-Liquid-Solid Mass Transfer Model for Taylor Flow in Micro (Milli) Channels: A Theoretical Approach and Experimental Proof. *Chem. Eng. J. Adv.* 4, 100065. doi:10.1016/j.cej.2020.100065
- Abolhasani, M., Kumacheva, E., and Günther, A. (2015). Peclet Number Dependence of Mass Transfer in Microscale Segmented Gas-Liquid Flow. *Ind. Eng. Chem. Res.* 54, 9046–9051. doi:10.1021/acs.iecr.5b01991
- Aboudheir, A., Tontiwachwuthikul, P., Chakma, A., and Idem, R. (2003). Kinetics of the Reactive Absorption of Carbon Dioxide in High CO<sub>2</sub>-loaded, Concentrated Aqueous Monoethanolamine Solutions. *Chem. Eng. Sci.* 58, 5195–5210. doi:10.1016/j.ces.2003.08.014
- Abu-Zahra, M. R. M., Schneiders, L. H. J., Niederer, J. P. M., Feron, P. H. M., and Versteeg, G. F. (2007). CO<sub>2</sub> Capture from Power Plants. Part I. A Parametric Study of the Technical Performance Based on Monoethanolamine. *Int. J. Greenh. Gas. Control* 1, 37–46. doi:10.1016/S1750-5836(06)00007-7
- Aghel, B., Heidaryan, E., Sahraie, S., and Nazari, M. (2018). Optimization of Monoethanolamine for CO<sub>2</sub> Absorption in a Microchannel Reactor. *J. CO<sub>2</sub> Util.* 28, 264–273. doi:10.1016/j.jcou.2018.10.005

## DATA AVAILABILITY STATEMENT

The original contributions presented in the study are included in the article/Supplementary Materials, further inquiries can be directed to the corresponding author.

## AUTHOR CONTRIBUTIONS

AA carried out the experiments and wrote the manuscript. MA conceived the original idea and designed the experimental set-up, bring up the fund, supervised the findings of the work, analyzed, write, and review the manuscript. AB verified the findings and provided critical feedback and reviewed the manuscript. JB carried out all the mathematical modeling work. All authors provided an equal contribution in discussing the result and commenting on the manuscript.

## FUNDING

This work was made possible by internal startup funding from Texas A&M University at Qatar and funding from UREP27-097-2-028 (Undergraduate Research Experience Program) from Qatar National Research Fund (QNRF).

## ACKNOWLEDGMENTS

The undergraduate students Ayaa Elidrisi, Omar Affifi, and Leela Elzayat are acknowledged for being present during experimental work and trained to carry out reactions on their own as part of UREP27-097-2-028.

- Aghel, B., Heidaryan, E., Sahraie, S., and Mir, S. (2019). Application of the Microchannel Reactor to Carbon Dioxide Absorption. *J. Clean. Prod.* 231, 723–732. doi:10.1016/j.jclepro.2019.05.265
- Aghel, B., Sahraie, S., and Heidaryan, E. (2020). Comparison of Aqueous and Non-aqueous Alkanolamines Solutions for Carbon Dioxide Desorption in a Microreactor. *Energy* 201, 117618. doi:10.1016/j.energy.2020.117618
- Al-Rawashdeh, M., Yu, F., Nijhuis, T. A., Rebrov, E. V., Hessel, V., and Schouten, J. C. (2012). Numbered-up Gas-Liquid Micro/milli Channels Reactor with Modular Flow Distributor. *Chem. Eng. J.* 207–208, 645–655. doi:10.1016/j.cej.2012.07.028
- Allhseinat, E., Pal, P., Keewan, M., and Banat, F. (2014). Foaming Study Combined with Physical Characterization of Aqueous MDEA Gas Sweetening Solutions. *J. Nat. Gas Sci. Eng.* 17, 49–57. doi:10.1016/j.jngse.2013.12.004
- Arachchige, U. S. P. R., Aryal, N., Eimer, D. A., and Melaaen, M. C. (2013). Viscosities of Pure and Aqueous Solutions of Monoethanolamine (MEA), Diethanolamine (DEA) and N-Methyldiethanolamine (MDEA). *Annu. Trans. Nord. Rheol. Soc.* 21, 299–306.
- Bangerth, S., Ganapathy, H., Ohadi, M., Khan, T. S., and Alshehhi, M. (2014). “Study of CO<sub>2</sub> Absorption into Aqueous Diethanolamine (Dea) Using Microchannel Reactors,” in *ASME International Mechanical Engineering Congress and Exposition, Proceedings (IMECE)* (American Society of Mechanical Engineers). doi:10.1115/IMECE2014-36348
- Berčić, G., and Pintar, A. (1997). The Role of Gas Bubbles and Liquid Slug Lengths on Mass Transport in the Taylor Flow through Capillaries. *Chem. Eng. Sci.* 52, 3709–3719. doi:10.1016/s0009-2509(97)00217-0

- Blauwhoff, P. M. M., Versteeg, G. F., and Van Swaaij, W. P. M. (1983). A Study on the Reaction between CO<sub>2</sub> and Alkanolamines in Aqueous Solutions. *Chem. Eng. Sci.* 38, 1411–1429. doi:10.1016/0009-2509(83)80077-3
- Cantu-Perez, A., Al-Rawashdeh, M. m., Hessel, V., and Gavriilidis, A. (2013). Reaction Modelling of a Microstructured Falling Film Reactor Incorporating Staggered Herringbone Structures Using Eddy Diffusivity Concepts. *Chem. Eng. J.* 227, 34–41. doi:10.1016/j.cej.2012.11.122
- Caplow, M. (1968). Kinetics of Carbamate Formation and Breakdown. *J. Am. Chem. Soc.* 90, 6795–6803. doi:10.1021/ja01026a041
- Cheung, O., Bacsik, Z., Liu, Q., Mace, A., and Hedin, N. (2013). Adsorption Kinetics for CO<sub>2</sub> on Highly Selective Zeolites NaKA and Nano-NaKA. *Appl. Energy* 112, 1326–1336. doi:10.1016/j.apenergy.2013.01.017
- Ganapathy, H., Shooshtari, A., Dessiatoun, S., Alshehhi, M., and Ohadi, M. M. (2013). Experimental Investigation of Enhanced Absorption of Carbon Dioxide in Diethanolamine in a Microreactor. Proceeding of the ASME 2013 11th International Conference on Nanochannels, Microchannels and Minichannels, ICNMM 2013, June 2013, Sapporo, Japan. American Society of Mechanical Engineers Digital Collection. doi:10.1115/ICNMM2013-73162
- Ganapathy, H., Steinmayer, S., Shooshtari, A., Dessiatoun, S., Ohadi, M. M., and Alshehhi, M. (2016). Process Intensification Characteristics of a Microreactor Absorber for Enhanced CO<sub>2</sub> Capture. *Appl. Energy* 162, 416–427. doi:10.1016/j.apenergy.2015.10.010
- Gupta, R., Fletcher, D. F., and Haynes, B. S. (2010). Taylor Flow in Microchannels: A Review of Experimental and Computational Work. *J. Comput. Multiph. Flows* 2, 1–31. doi:10.1260/1757-482x.2.1.1
- Haase, S., Murzin, D. Y., and Salmi, T. (2016). Review on Hydrodynamics and Mass Transfer in Minichannel Wall Reactors with Gas-Liquid Taylor Flow. *Chem. Eng. Res. Des.* 113, 304–329. doi:10.1016/j.cherd.2016.06.017
- Hartman, R. L., and Jensen, K. F. (2009). Microchemical Systems for Continuous-Flow Synthesis. *Lab. Chip* 9, 2495–2507. doi:10.1039/b906343a
- Hessel, V., Knobloch, C., and Lowe, H. (2008). Review on Patents in Microreactor and Micro Process Engineering. *Cheng* 1, 1–16. doi:10.2174/2211334710801010001
- IPCC (2014). *Climate Change 2014: Synthesis Report. Contribution of Working Groups I, II and III to the Fifth Assessment Report of the Intergovernmental Panel on Climate Change.*
- Korson, L., Drost-Hansen, W., and Millero, F. J. (1969). Viscosity of Water at Various Temperatures. *J. Phys. Chem.* 73, 34–39. doi:10.1021/j100721a006
- Lefortier, S. G. R., Hamersma, P. J., Bardow, A., and Kreutzer, M. T. (2012). Rapid Microfluidic Screening of CO<sub>2</sub> Solubility and Diffusion in Pure and Mixed Solvents. *Lab. Chip* 12, 3387–3391. doi:10.1039/c2lc40260b
- Li, L., Maeder, M., Burns, R., Puxty, G., Clifford, S., and Yu, H. (2017). The Henry Coefficient of CO<sub>2</sub> in the MEA-CO<sub>2</sub>-H<sub>2</sub>O System. *Energy Procedia* 114, 1841–1847. doi:10.1016/j.egypro.2017.03.1313
- Liang, Z., Rongwong, W., Liu, H., Fu, K., Gao, H., Cao, F., et al. (2015). Recent Progress and New Developments in Post-combustion Carbon-Capture Technology with Amine Based Solvents. *Int. J. Greenh. Gas Control* 40, 26–54. doi:10.1016/j.jggc.2015.06.017
- Maqsood, K., Mullick, A., Ali, A., Kargupta, K., and Ganguly, S. (2014). Cryogenic Carbon Dioxide Separation from Natural Gas: A Review Based on Conventional and Novel Emerging Technologies. *Rev. Chem. Eng.* 30, 453–477. doi:10.1515/revce-2014-0009
- Mason, B. P., Price, K. E., Steinbacher, J. L., Bogdan, A. R., and McQuade, D. T. (2007). Greener Approaches to Organic Synthesis Using Microreactor Technology. *Chem. Rev.* 107, 2300–2318. doi:10.1021/cr050944c
- McMullen, J. P., and Jensen, K. F. (2010a). An Automated Microfluidic System for Online Optimization in Chemical Synthesis. *Org. Process Res. Dev.* 14, 1169–1176. doi:10.1021/op100123e
- McMullen, J. P., and Jensen, K. F. (2010b). Integrated Microreactors for Reaction Automation: New Approaches to Reaction Development. *Annu. Rev. Anal. Chem.* 3, 19–42. doi:10.1146/annurev.anchem.111808.073718
- Nwaoha, C., Saiwan, C., Tontiwachuthikul, P., Supap, T., Rongwong, W., Idem, R., et al. (2016). Carbon Dioxide (CO<sub>2</sub>) Capture: Absorption-Desorption Capabilities of 2-Amino-2-Methyl-1-Propanol (AMP), Piperazine (PZ) and Monoethanolamine (MEA) Tri-solvent Blends. *J. Nat. Gas Sci. Eng.* 33, 742–750. doi:10.1016/j.jngse.2016.06.002
- Ramezani, R., Mazinani, S., and Di Felice, R. (2019). A Comprehensive Kinetic and Thermodynamic Study of CO<sub>2</sub> Absorption in Blends of Monoethanolamine and Potassium Lysinate: Experimental and Modeling. *Chem. Eng. Sci.* 206, 187–202. doi:10.1016/j.ces.2019.05.039
- Reizman, B. J., and Jensen, K. F. (2016). Feedback in Flow for Accelerated Reaction Development. *Acc. Chem. Res.* 49, 1786–1796. doi:10.1021/acs.accounts.6b00261
- Sada, E., Kumazawa, H., and Butt, M. A. (1978). Solubility and Diffusivity of Gases in Aqueous Solutions of Amines. *J. Chem. Eng. Data* 23, 161–163. doi:10.1021/je60077a008
- Sedransk Campbell, K. L., Lapidot, T., and Williams, D. R. (2015). Foaming of CO<sub>2</sub>-Loaded Amine Solvents Degraded Thermally under Stripper Conditions. *Ind. Eng. Chem. Res.* 54, 7751–7755. doi:10.1021/acs.iecr.5b01935
- Shao, N., Gavriilidis, A., and Angeli, P. (2009). Flow Regimes for Adiabatic Gas-Liquid Flow in Microchannels. *Chem. Eng. Sci.* 64, 2749–2761. doi:10.1016/j.ces.2009.01.067
- Shokrollahi, F., Lau, K. K., Partoon, B., and Smith, A. M. (2022). A Review on the Selection Criteria for Slow and Medium Kinetic Solvents Used in CO<sub>2</sub> Absorption for Natural Gas Purification. *J. Nat. Gas Sci. Eng.* 98, 104390. doi:10.1016/J.JNGSE.2021.104390
- Sobieszuk, P., Ilnicki, F., and Pohorecki, R. (2014). Contribution of Liquid- and Gas-Side Mass Transfer Coefficients to Overall Mass Transfer Coefficient in Taylor Flow in a Microreactor. *Chem. Process Eng. - Inz. Chem. i Proces.* 35, 35–45. doi:10.2478/cpe-2014-0003
- Thitakamol, B., Veawab, A., and Aroonwilas, A. (2009). Foaming in Amine-Based CO<sub>2</sub> Capture Process: Experiment, Modeling and Simulation. *Energy Procedia* 1, 1381–1386. doi:10.1016/j.egypro.2009.01.181
- Thitakamol, B., and Veawab, A. (2008). Foaming Behavior in CO<sub>2</sub> Absorption Process Using Aqueous Solutions of Single and Blended Alkanolamines. *Ind. Eng. Chem. Res.* 47, 216–225. doi:10.1021/ie070366l
- Tobiesen, F. A., Svendsen, H. F., and Hoff, K. A. (2005). Desorber Energy Consumption Amine Based Absorption Plants. *Int. J. Green Energy* 2, 201–215. doi:10.1081/ge-200058981
- Vandu, C. O., Liu, H., and Krishna, R. (2005). Mass Transfer from Taylor Bubbles Rising in Single Capillaries. *Chem. Eng. Sci.* 60, 6430–6437. doi:10.1016/j.ces.2005.01.037
- Venna, S. R., and Carreon, M. A. (2015). Metal Organic Framework Membranes for Carbon Dioxide Separation. *Chem. Eng. Sci.* 124, 3–19. doi:10.1016/j.ces.2014.10.007
- Versteeg, G. F., Blauwhoff, P. M. M., and van Swaaij, W. P. M. (1987). The Effect of Diffusivity on Gas-Liquid Mass Transfer in Stirred Vessels. Experiments at Atmospheric and Elevated Pressures. *Chem. Eng. Sci.* 42, 1103–1119. doi:10.1016/0009-2509(87)80060-X
- Versteeg, G. F., Van Dijk, L. A. J., and Van Swaaij, W. P. M. (1996). ON THE KINETICS BETWEEN CO<sub>2</sub> AND ALKANOLAMINES Both IN AQUEOUS AND NON-AQUEOUS SOLUTIONS. AN OVERVIEW. *Chem. Eng. Commun.* 144, 113–158. doi:10.1080/00986449608936450
- Versteeg, G. F., and Van Swaaij, W. P. M. (1988). Solubility and Diffusivity of Acid Gases (Carbon Dioxide, Nitrous Oxide) in Aqueous Alkanolamine Solutions. *J. Chem. Eng. Data* 33, 29–34. doi:10.1021/je00051a011
- Wang, M., Joel, A. S., Ramshaw, C., Eimer, D., and Musa, N. M. (2015). Process Intensification for Post-combustion CO<sub>2</sub> Capture with Chemical Absorption: A Critical Review. *Appl. Energy* 158, 275–291. doi:10.1016/j.apenergy.2015.08.083
- Wirth, T. (2013). *Microreactors in Organic Chemistry and Catalysis*. Second Edition. Wiley VCH. doi:10.1002/9783527659722
- Yao, C., Zhu, K., Liu, Y., Liu, H., Jiao, F., and Chen, G. (2017). Intensified CO<sub>2</sub> Absorption in a Microchannel Reactor under Elevated Pressures. *Chem. Eng. J.* 319, 179–190. doi:10.1016/j.cej.2017.03.003
- Yao, C., Zhao, Y., Ma, H., Liu, Y., Zhao, Q., and Chen, G. (2021). Two-phase Flow and Mass Transfer in Microchannels: A Review from Local Mechanism to Global Models. *Chem. Eng. Sci.* 229, 116017. doi:10.1016/j.ces.2020.116017
- Ye, C., Dang, M., Yao, C., Chen, G., and Yuan, Q. (2013). Process Analysis on CO<sub>2</sub> Absorption by Monoethanolamine Solutions in Microchannel Reactors. *Chem. Eng. J.* 225, 120–127. doi:10.1016/j.cej.2013.03.053

- Yue, J., Chen, G., Yuan, Q., Luo, L., and Gonthier, Y. (2007). Hydrodynamics and Mass Transfer Characteristics in Gas-Liquid Flow through a Rectangular Microchannel. *Chem. Eng. Sci.* 62, 2096–2108. doi:10.1016/j.ces.2006.12.057
- Yue, J., Luo, L., Gonthier, Y., Chen, G., and Yuan, Q. (2009). An Experimental Study of Air-Water Taylor Flow and Mass Transfer inside Square Microchannels. *Chem. Eng. Sci.* 64, 3697–3708. doi:10.1016/j.ces.2009.05.026
- Zhu, C., Li, C., Gao, X., Ma, Y., and Liu, D. (2014). Taylor Flow and Mass Transfer of CO<sub>2</sub> Chemical Absorption into MEA Aqueous Solutions in a T-Junction Microchannel. *Int. J. Heat Mass Transf.* 73, 492–499. doi:10.1016/j.ijheatmasstransfer.2014.02.040

**Conflict of Interest:** The authors declare that the research was conducted in the absence of any commercial or financial relationships that could be construed as a potential conflict of interest.

**Publisher's Note:** All claims expressed in this article are solely those of the authors and do not necessarily represent those of their affiliated organizations, or those of the publisher, the editors and the reviewers. Any product that may be evaluated in this article, or claim that may be made by its manufacturer, is not guaranteed or endorsed by the publisher.

*Copyright © 2022 Ashok, Ballout, Benamor and Al-Rawashdeh. This is an open-access article distributed under the terms of the Creative Commons Attribution License (CC BY). The use, distribution or reproduction in other forums is permitted, provided the original author(s) and the copyright owner(s) are credited and that the original publication in this journal is cited, in accordance with accepted academic practice. No use, distribution or reproduction is permitted which does not comply with these terms.*